Ecosystems
https://doi.org/10.1007/s10021-019-00387-5

ECOSYSTEMS

Applying Climate Change Risk Management Tools to Integrate Streamflow Projections and Social Vulnerability

Sheila M. Saia,[1,2,3]* Kelly M. Suttles,[4] Bethany B. Cutts,[5,6] Ryan E. Emanuel,[3,6] Katherine L. Martin,[3,6] David N. Wear,[2] John W. Coulston,[7] and James M. Vose[2]

[1]*Oak Ridge Institute for Science and Education, Oak Ridge, Tennessee, USA;* [2]*United States Department of Agriculture Forest Service Southern Research Station, 3041 East Cornwallis Road, Durham, North Carolina 27709, USA;* [3]*Department of Forestry and Environmental Resources, North Carolina State University, Raleigh, North Carolina, USA;* [4]*Center for Housing and Community Studies, University of North Carolina at Greensboro, Greensboro, North Carolina, USA;* [5]*Department of Tourism, Parks and Management, North Carolina State University, Raleigh, North Carolina, USA;* [6]*Center for Geospatial Analytics, North Carolina State University, Raleigh, North Carolina, USA;* [7]*United States Department of Agriculture Forest Service Southern Research Station, Blacksburg, Virginia, USA*

Abstract

Shifts in streamflow, due to future climate and land use change, may pose risks to nearby human communities. Projecting the spatial distribution and impacts of these risks requires consideration of biophysical and socioeconomic factors. Models like the Soil and Water Assessment Tool (SWAT) can project spatial distributions of hydrologic risk due to shifting biophysical factors like climate and land use, but cannot account for socioeconomic factors influencing a community's capacity to adapt to future streamflow changes. To address this limitation, we used a risk matrix to classify subbasins in a large river basin in the southeastern USA based on (1) percent increase in SWAT simulated 10-year and extreme high flows due to climate and land use change between baseline (1982–2002) and projected (2050–2070) periods and (2) degree of community vulnerability according to a Social Vulnerability Index (SVI). We compared spatial distributions of high-risk subbasins based on SWAT results, SVI results, and the integration of SWAT and SVI results using a risk matrix. Large increases in simulated 10-year and extreme high flows occurred in middle and lower parts of the river basin, and socially vulnerable communities were distributed throughout. We identified 16, 7, and 14 unique high-risk subbasins using SWAT results, SVI results, and SWAT and SVI results, respectively. By using a risk matrix, we identified subbasins with vulnerable communities that are projected to experience future increases in streamflow due to climate and land use change. These results serve as a starting point for subsequent climate change adaptation planning.

Key words: climate change; adaptation planning; land use change; social vulnerability; soil water assessment tool; water resources.

Received 7 December 2018; accepted 22 March 2019

Electronic supplementary material: The online version of this article (https://doi.org/10.1007/s10021-019-00387-5) contains supplementary material, which is available to authorized users.

Author Contributions SMS, KMS, JMV, REE, and DNW designed the study. SMS performed the research and analyzed the data. All authors interpreted the data. SMS drafted the manuscript and prepared data and code for GitHub/Zenodo. All authors provided critical revision.

**Corresponding author; e-mail:* ssaia@ncsu.edu

Published online: 15 May 2019

Highlights

- Identifying vulnerable human communities is critical for climate change planning.
- We used a risk matrix to link projected streamflow with socioeconomic metrics.
- This risk matrix approach identified unique high-risk subbasins.

Introduction

Concurrent regional increases in future precipitation (for example, Walsh and others 2014; Hayhoe and others 2018) and urban development (for example, Terando and others 2014) may lead to larger and more frequent streamflow peaks (Ogden and others 2011; Walsh and others 2014; Martin and others 2017; Ficklin and others 2018; Hayhoe and others 2018; Suttles and others 2018). These shifts in streamflow magnitude and frequency may increase the risk of adverse social and economic consequences on nearby communities (Emrich and Cutter 2011; IPCC 2014; Hsiang and others 2017). Risk management tools—like a risk matrix (Raiffa and Schlaiffer 2000; Major and O'Grady 2010; Schwartz 2010; Yohe 2010; Yohe and Leichenko 2010; Ojima and others 2014; Schwartz and others 2014)—may help plan for and mitigate risk by linking the likelihood of an event (for example, high or extreme streamflow) with the capacity for a community to bear the consequences of that event. Therefore, there is a need for risk management tools that incorporate (1) biophysical factors altering future streamflow and (2) socioeconomic factors influencing whether communities are capable of adapting to future changes in streamflow.

Hydrologic models and socioeconomic metrics have a limited ability to account for both biophysical and socioeconomic factors independently. More specifically, the Soil and Water Assessment Tool (SWAT; Arnold and others 1998; Neitsch and others 2011) is a physically based hydrologic model used by researchers across the globe to project the impacts of future climate and land use change on water resources (Lee and Chung 2007; Ma and others 2010; Kim and others 2014; Krysanova and Srinivasan 2014; Natkhin and others 2015; Hovenga and others 2016; Ahiablame and others 2017; Suttles and others 2018). Technical information derived from SWAT has helped inform local, regional, and national water resource management such as managing land use transitions, resizing culverts and ditches, and developing drought management/water conservation plans (Gassman and others 2007; Francesconi and others 2016; FEMA 2018). SWAT can simulate the impact of biophysical factors such as future climate and land use change on streamflow. However, SWAT does not incorporate socioeconomic data; thus, it has a limited ability to address socioeconomic outcomes.

Socioeconomic metrics such as Social Vulnerability Indices (SVIs) may serve as a starting point to identify vulnerable communities—communities with limited resources to prepare, respond, recover, and adapt to environmental hazards (Cutter and others 2003; Flanagan and others 2011)—that may experience adverse consequences due to future increases in streamflow. SVIs are spatially explicit, quantitative measures that are calculated using human population data from government sources like the United States Census Bureau American Community Survey (ACS; https://www.census.gov/programs-surveys/acs/). SVIs include a number of socioeconomic variables that encompass themes of personal wealth, age, housing type, density, housing ownership, race, ethnicity, and occupation (Cutter and others 2003; Flanagan and others 2011). There are many different formulations of SVI with some being more complex (for example, Cutter and others 2003) than others (for example, Flanagan and others 2011), but the larger the SVI, the more vulnerable the spatial unit (for example, census tract). SVIs have been used to study the persistence and creation of social vulnerability in space and time as well as to study the potential impacts of environmental hazards on communities around the world (Cutter and others 2003; Cutter and Finch 2008; Finch and others 2010; Emrich and Cutter 2011; Flanagan and others 2011; Guillard-Gonçalves and others 2015; KC and others 2015; Cutts and others 2018). However, SVIs do not consider the impact of shifting biophysical factors on streamflow. We use the SVI developed by Flanagan and others (2011), which is publicly available for the continental USA on the Centers for Disease Control Agency for Toxic Substances and Disease Registry (CDC-ATSDR) website (https://svi.cdc.gov/), to characterize social vulnerability for our study area.

A risk matrix (Raiffa and Schlaiffer 2000; Major and O'Grady 2010; Schwartz 2010; Yohe 2010; Yohe and Leichenko 2010; Ojima and others 2014; Schwartz and others 2014) offers a framework for combining SWAT and SVI results to identify areas (that is, watersheds or subbasins) that are at high-risk of experiencing large shifts in future streamflow and also contain communities with limited

capacity to bear the consequences of these shifts. Previous research used a risk matrix approach to inform climate change adaptation and mitigation planning in New York City, New York, USA (Major and O'Grady 2010; Yohe 2010; Yohe and Leichenko 2010; Schwartz and others 2014). Others have used a risk matrix to manage wildlife habitats, forest carbon stocks, and forest fires under changing climate regimes (Iverson and others 2012; Woodall and others 2013; Ojima and others 2014). Here, we use a risk matrix to inform climate change adaptation planning as it relates to water resources management.

Given projected shifts in streamflow due to climate and land use change as well as the need to identify and support vulnerable communities as they adapt to these future shifts in streamflow, we asked the following research question: *How does combining SWAT and SVI results using a risk matrix affect the identification of high-risk subbasins compared to using SWAT and SVI results alone?* To answer this question, we compared the spatial distribution of high-risk subbasins in the Yadkin–Pee Dee River Watershed (YPD), North Carolina, USA, based on three approaches: (1) SWAT results for 10-year and extreme high flows (2) SVI results, and (3) the integration of SWAT and SVI results using a risk matrix. Although we address this research question in the YPD, a similar approach could be applied to other regions where baseline streamflow, projected streamflow, and SVI results are available.

Methods

Site Description

Our study site is located in the YPD, which spans western and central North Carolina (NC), USA, and has an area of 17,780 km^2 (Figure 1). The observed average annual temperature and precipitation (± standard deviation) from the 1982–2002 baseline period for the YPD were 19.7 (± 9.5) °C and 1185 (± 167) mm y^{-1}, respectively. In 1992—the midpoint of baseline period—the YPD was 65% forested (that is, lowland and upland hardwoods, pines, and mixed forest), 17% non-stocked (that is, forested stands with < 17% growing stock trees), 11% agriculture, 6% developed, and 1% wetlands and water bodies (Vogelmann and others 2001). A total of 27 counties and 456 census tracks lie either partially or completely within the YDP. The 5-year ACS population estimate for the YPD from 2010 to 2014 was about 1.66 million (Table 1). The YDP includes the suburbs of Charlotte, NC in Mecklenburg and Union Counties, the city of Winston-Salem, NC, in Forsyth County, and a number of other smaller cities and towns (Table S1). The populations of Mecklenburg, Union, and Forsyth Counties are projected to grow by 115–229 people km^{-2} (50–100 people mi^{-2}), whereas other regions of the YPD are projected to either grow or stay the same by 2060. Very few counties in the YPD are projected to decline in population (USFS 2012; Wear and others 2013). For additional description of the YPD, see Suttles and others (2018).

We chose the YPD as a test case for two reasons. First, previous research indicates that climate and land use change will likely impact water resources and communities in this region (Martin and others 2017; Suttles and others 2018). Climate change projections include a 2.2–6.6 °C increase in annual temperature in the Southeast United States (SEUS) by 2100 (Kunkel and others 2013). Precipitation patterns in the SEUS, although less certain than temperature estimates (Fekete and others 2004; Kunkel and others 2013; McNulty and others 2013; Carter and others 2014; Walsh and others 2014), are projected to be more extreme and will likely result in more intense rainfall events with longer periods between these events (O'Gorman and Schneider 2009; Laseter and others 2012; IPCC 2014; Walsh and others 2014; Carter and others 2018). Population growth and subsequent urban land cover in the SEUS are expected to increase 101–192% by 2060 (Terando and others 2014), and associated impervious cover may exacerbate high streamflow events by increasing peak flows and reducing groundwater recharge (Ogden and others 2011; Hamel and others 2013; Walsh and others 2014; Martin and others 2017; Carter and others 2018; Ficklin and others 2018; Suttles and others 2018). Second, the YPD contains communities that are likely to be vulnerable to environmental hazards associated with high streamflow. Approximately 17% of the population in the YPD lives below the poverty line (Table 1).

Hydrologic Model

This study relies on the previous work of Suttles and others 2018, who developed a SWAT for the YPD. According to standard hydrologic model evaluation criteria (Moriasi and others 2007), the SWAT simulated daily streamflow well; results ranged from satisfactory to very good (Suttles and others 2018). A total of 28 subbasins were delineated by SWAT (Figure 1); the number of subbasins is based on parameterization and computational efficiency. In this study, we used climate and land use data as inputs into the SWAT

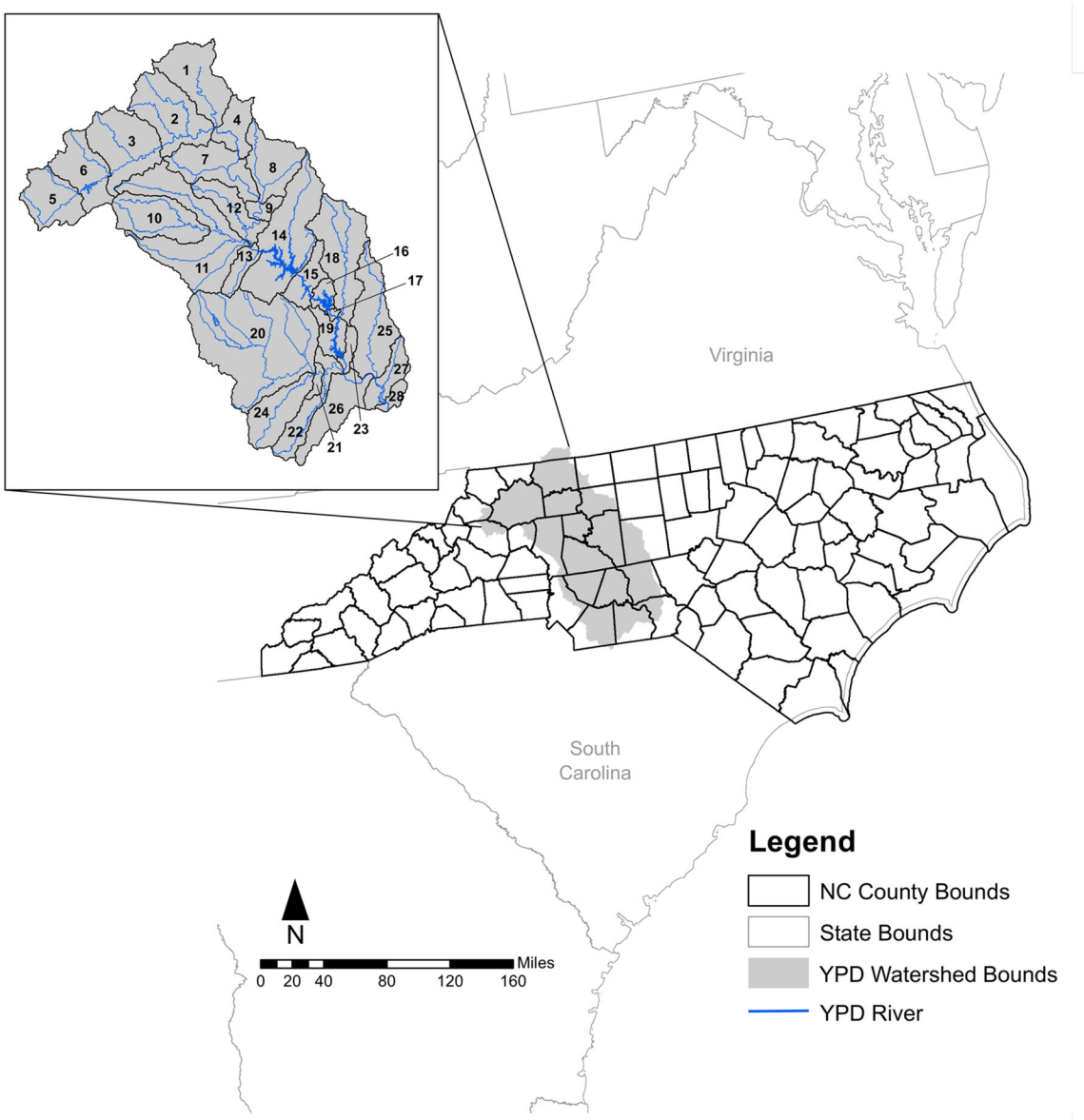

Figure 1. Spatial extent of the Yadkin–Pee Dee River (YPD) Watershed in North Carolina (NC), USA. Inset shows the YPD and numbers corresponding to subbasin IDs as assigned by the Soil and Water Assessment Tool (SWAT) (Color figure online).

to simulate daily streamflow for baseline (1982–2002) and projected (2050–2070) periods across an envelope of four future climate–land use change scenarios (referred to henceforth as future scenarios). These four scenarios paired three unique general circulation models (GCMs; that is, MIROC, CSIRO, and Hadley), with either rapid (that is, RCP 8.5) or moderate (that is, RCP 4.5) increases in greenhouse gas emissions (IPCC 2014), and land use change projections. Further detail of these four future scenarios is summarized in Table 2 and described in Suttles and others (2018).

As described by Suttles and others (2018), we downloaded downscaled MIROC, CSIRO, and Hadley climate variables (that is, precipitation, temperature, solar radiation, relative humidity, and wind speed) for the baseline period and used these as inputs into the SWAT to simulate baseline daily streamflow. This process of simulating baseline streamflow from (historic) GCM climate variables is known as *backcasting*. Backcasting reduces uncertainty by ensuring that differences between past and future streamflow are due to model inputs alone rather than model inputs and differences

Table 1. Description and Yadkin–Pee Dee River watershed (YPD) values of the 15 American Community Survey (ACS) 2010–2014 variables used to calculate the Social Vulnerability Index (SVI) in this study

Number	ACS variable description	YPD value
1	Number of people below the poverty line	275,000 (6350)
2	Number of civilian (age 16 or older) unemployed	89,300 (2370)
3	Per capita income	$19,700 (158)
4	Number of people (age 25 or older) with no high school diploma	17,7000 (3330)
5	Number of people age 65 or older	23,1000 (2340)
6	Number of people age 17 or younger	399,000 (4450)
7	Number of civilian non-institutionalized people with a disability	211,000 (3290)
8	Number of single parent households with children under age 18	62,100 (1770)
9	Number of non-white, non-Hispanic people	511,000 (11,100)
10	Number of people (age 5 or older) who speak English ''less than well''	45,400 (2310)
11	Number of housing structures with 10 or more units	50,200 (1540)
12	Number of mobile homes	88,300 (1880)
13	Number of housing units with more people than rooms	15,800 (960)
14	Number of households with no vehicle	37,800 (1290)
15	Number of institutionalized people in group quarters	36,100 (1680)

The total population estimate for the YPD is ~ 1.66 million ± a margin of error (MOE) of 8350 people. Values in parenthesis represent the MOE as defined in USCB (2008).

Table 2. Average increases in temperature and precipitation from backcast baseline to projected future scenarios included in this study

Future scenario	Temperature increase (°C)	Precipitation increase (mm year^{-1})	Land use scenario
MIROC 8.5	3.2	146	High timber prices, 60% increase in population and income
CSIRO 8.5	2.7	131	Low timber prices, 60% increase in population and income
CSIRO 4.5	2.4	219	High timber prices, 40% increase in population and income
Hadley 4.5	3.5	73	Low timber prices, 40% increase in population and income

This table was adapted from Suttles and others (2018). Corresponding land use scenarios originate from the United States Department of Agriculture Forest Service (USFS) Southern Forest Futures Project (Wear 2013; Wear and others 2013).

caused by how the model represents reality (Quist and Vergragt 2006; Van der Voorn and others 2012). Backcast GCM annual average, 10th, and 90th percentiles of daily streamflow were smaller than observations (Table S2, Figure S1). For the projected period, we downloaded downscaled MIROC RCP 8.5, CSIRO RCP 8.5, CSIRO RCP 4.5, and Hadley RCP 4.5 climate variables and used these as inputs into the SWAT to simulate projected daily streamflow. See Suttles and others (2018) for further details related to the climate data used in this study.

We represented baseline land use conditions using the 1992 National Land Cover Dataset (NLCD; Vogelmann and others 2001) and used projected land use data from the United States Department of Agriculture Forest Service (USFS) Southern Forest Futures Project (USFS 2012; Wear 2013; Wear and others 2013). More specifically, the Southern Forest Futures Project incorporates future changes in population growth, income growth, and timber prices for the YPD (Table 2). As timber prices are influential in the distribution of forest land use across the SEUS (USFS 2012; Wear 2013), land use change scenarios pair high and low timber prices across future scenarios with either 60% population and income growth or 40% population and income. USFS (2012), Wear (2013), and Martin and others (2017) provide further details on the assumptions governing timber prices, population, and income for the land use projections used here.

Streamflow Analysis

We implemented standard cumulative annual maximum log-Pearson Type III streamflow frequency analyses (IACWD 1982) to estimate 10-year (24-h) high flows from SWAT simulated daily

streamflow. For the purpose of this study, we focused on 10-year high flows because they are commonly used for stormwater infrastructure design (USEPA 2009). However, this analysis could be repeated for low flows as well as alternative return periods depending on the goals of the climate change adaptation planning project. We determined the baseline period 10-year high flow cutoff (F_{10}) for a corresponding 10-year (24-h) return period and calculated the percent change PC_{10} in number of days per year where streamflow was ≥ F_{10} using equation (1):

$$PC_{10} = \frac{\frac{n_{p,10} - n_{b,10}}{n_{b,10}} * 100}{n_s} \quad (1)$$

where $n_{b,10}$ and $n_{p,10}$ represent the number of days where streamflow was ≥ F_{10} in the baseline and projection datasets, respectively, and n_s is equal to number of simulation years (that is, 20). Thus, PC_{10} reflects either an increase or decrease in the frequency of 10-year (or greater) high flows (per year) between the baseline and projected periods.

In addition to 10-year high flow analysis, we included extreme high flow analysis as a secondary way to present SWAT results; these events pose the highest risk of flooding to communities. We defined extreme flows as synonymous with minor outliers, that is, when SWAT simulated daily streamflow was ≥ the baseline extreme flow cutoff (F_{ext}) given in equation (2).

$$F_{ext} = Q_3 + 1.5(Q_3 - Q_1) \quad (2)$$

where Q_1 and Q_3 are the 25th (first quartile) and 75th (third quartile) percentiles of streamflow, respectively. We log-transformed baseline and projected streamflow, calculated F_{ext} from the baseline dataset for each subbasin, and determined the percent change (PC_{ext}) in number of days per year where streamflow was ≥ F_{ext} using equation (3):

$$PC_{ext} = \frac{\frac{n_{p,ext} - n_{b,ext}}{n_{b,ext}} * 100}{n_s} \quad (3)$$

where $n_{b,ext}$ and $n_{p,ext}$ represent the number of days where streamflow was ≥ F_{ext} in the baseline and projection datasets, respectively. Thus, PC_{ext} reflects either an increase or decrease in the frequency of extreme high flows (per year) between the baseline and projected periods.

Social Vulnerability Index

We used the census tract SVI available online at the Centers for Disease Control Agency for Toxic Substances and Disease Registry (CDC-ATSDR) website (https://svi.cdc.gov/). Flanagan and others (2011) derived these SVIs from 2010 to 2014 ACS data (https://www.census.gov/programs-surveys/acs). Descriptions of the ACS variables included in the CDC-ATSDR SVI are shown in Table 1. The SVI as determined by Flanagan and others (2011) is the sum of ranked percentiles for each variable relative to all census tracts in the continental USA; thus, a SVI of 15 represents the most vulnerable census tract in the continental USA, whereas a SVI close to 0 represents the least vulnerable. In the YPD, each census tract represents 4300 people on average (USCB 2008). We did not project social vulnerability (see ''Future Directions'' section for further discussion on the implications and future directions of this work).

To compare census tract SVI data to subbasin SWAT results, we scaled census tract SVIs to each subbasin using an area weighted average approach. There were two major reasons why we scaled census tract SVI data to each subbasin—rather than scaling SWAT data to the census tract. First, it is beneficial to manage water resources at the watershed scale (Molle 2009; Cutts and others 2018). Second, we assumed that less uncertainty would be introduced when scaling up higher resolution, census tract SVI results compared to scaling down lower resolution, subbasin SWAT results. We determined the subbasin SVI using equation (4):

$$SVI_i = \sum_{j=1}^{N} \left(\frac{CA_j}{SA_i} \right) SVI_j \quad (4)$$

where i represents a given subbasin (i ranged from 1 to 28) and j represents a census tract within subbasin i (j ranges from 1 to N; N is equal to the total number of census tracts within subbasin i), CA_j represents the area of census tract j within subbasin i, SA_i represents the area of subbasin i, and SVI_j represents the SVI of census tract j within subbasin i. For each subbasin, we calculated SA_i and then used the subbasin boundary to mask census tract SVI spatial data. From this masked census tract SVI output, we identified each census tract SVI value (each SVI_j) within the subbasin and calculated each CA_j. We used the arcpy Python library in ArcGIS to automate these calculations for all 28 subbasins. We also recorded the maximum census tract SVI within each subbasin and used this—along with the subbasin SVI—to classify risk for the SWAT and SVI approach. See ''Social Vulnerability'' section for further discussion on why we used both scales.

We calculated area weighted cumulative density functions (CDFs) using the following approach. First, we ordered census tract SVIs with a particular subbasin from low to high and multiplied each census tract SVI by its fraction of total subbasin area; this resulted in an ordered list of area weighted census tract SVIs. The ordered list ranged from rank = 1 to rank = N (see equation (1)). Next, we iteratively calculated the cumulative sum of area weighted census tract SVIs for each rank (from rank 1 up to and including the given rank) and divided each cumulative sum by the corresponding subbasin SVI as calculated by equation (1). This resulted in an area weighted CDF value for each ranked census tract SVI. We repeated this approach for each subbasin. Besides plotting CDFs, we used a Kolmogorov–Smirnov (KS) test to compare the distributions of census tract SVIs in the USA, NC, and YPD. CDF calculations and KS tests were done in R.

Comparison of Approaches

To address our research question, we mapped the spatial distribution of high-risk subbasins based on three approaches: SWAT results, SVI results, and the integration of SWAT and SVI results using a risk matrix. See below for details on each approach. For all three approaches, we used yellow, orange, and red to represent subbasins with low, medium, and high-risks, respectively. For the SWAT results map, low-risk subbasins had PC_{10} and PC_{ext} that were $\leq$ 25%, medium-risk subbasins had PC_{10} and PC_{ext} that were $>$ 25% or $\leq$ 50%, and high-risk subbasins had PC_{10} and PC_{ext} that were $>$ 50% (Figure S2a). To summarize high-risk SWAT results across the four future scenarios, we labeled a subbasin as high-risk in the summary when it was identified as high-risk in at least one of the four future scenarios. For example, using this summary approach, we generated Figure 4B from the high-risk results presented in Figure S3 and generated Figure 4D from the high-risk results presented in Figure S4.

For the SVI results map, low-risk subbasins either had a subbasin SVI or census tract SVI within the subbasin that was $\leq$ 9.6 (that is, first standard deviation of all continental USA census tract SVIs), medium-risk subbasins either had a subbasin SVI or a census track SVI within the subbasin that was $>$ 9.6 or $\leq$ 11.8 (that is, second standard deviation of all continental USA census tract SVIs), and high-risk subbasins had either a subbasin SVI or a census tract SVI within the subbasin that was $>$ 11.8 (Figure S2b). We used these cutoffs because they were statistically intuitive and also reflected the social vulnerability within the YPD compared to the entire USA. We generated Figure 4A from the high-risk results in Figure S5. We used both subbasin (low-resolution) and census tract (high-resolution) scales to account for spatial heterogeneity in social vulnerability. See ''Social Vulnerability'' section for further discussion on why we included both scales.

To integrate SWAT and SVI results and generate associated maps, we adapted a risk matrix (Raiffa and Schlaiffer 2000; Schwartz 2010; Schwartz and others 2014; Yohe 2010; Yohe and Leichenko 2010; Iverson and others 2012; Woodall and others 2013; Ojima and others 2014) to classify both SWAT and SVI results in the YPD (Figure 2). We defined *risk* as the product of the likelihood of impact of a streamflow event and the capacity for a community to bear the consequences of that event. We used PC_{10} and PC_{ext} to represent the *likelihood of impact* (x axis, Figure 2). We assumed subbasins with percent change values above zero were more likely to experience a large increase in 10-year and extreme high flows in the future. We used the area weighted subbasin SVI and the maximum census tract SVI within a given subbasin to represent the *capacity to bear the consequences* of a streamflow event (y axis, Figure 2). Thus, we assumed socioeconomic consequences were greater for

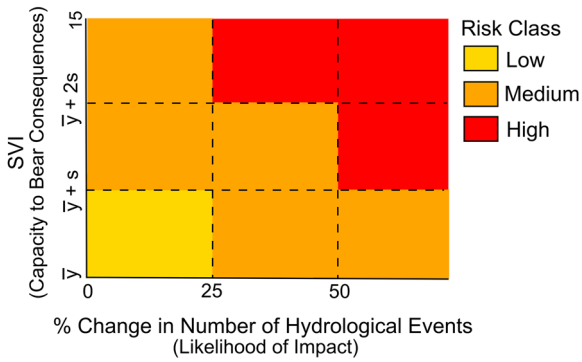

Figure 2. Risk matrix used to classify the census tract and subbasin Social Vulnerability Index (SVI) values as well as the percent change in Soil and Water Assessment Tool (SWAT) 10-year and extreme high flow events for subbasins in the Yadkin–Pee Dee River Watershed. The y axis cutoff variables $\bar{y}$, $\bar{y} + s$, and $\bar{y} + 2s$ represent the mean (7.3), first standard deviation (9.6), and second standard deviation (11.8), respectively, of all census tract SVIs in the continental USA. This figure was adapted from Yohe (2010) and Iverson and others (2012) (Color figure online).

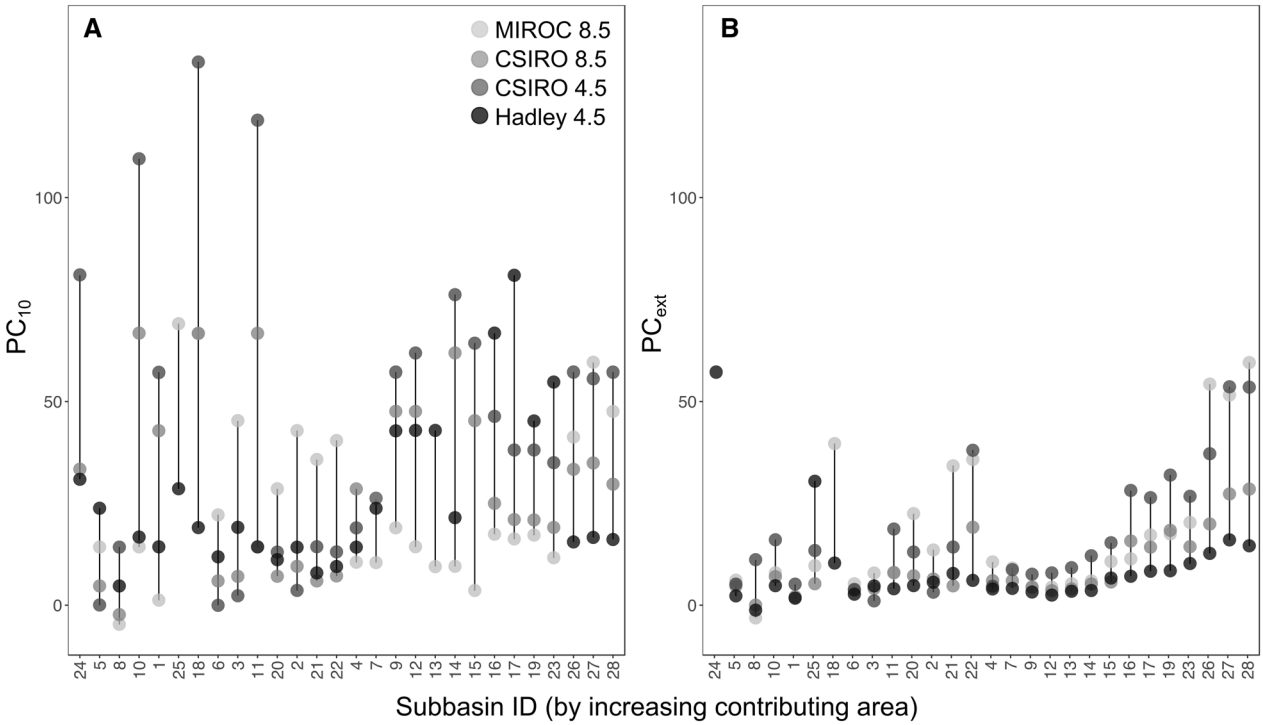

Figure 3. Variation in **A** percent change (PC_{10}) in number of days per year where streamflow was ≥ F_{10} between the baseline and projected datasets and **B** percent change (PC_{ext}) in number of days per year where streamflow was ≥ F_{ext} between the baseline and projected datasets versus SWAT subbasin identification number ordered by increasing contributing area for each of the four future scenarios. Vertical lines denote the range of outputs.

communities that are unable to prepare for, respond to, recover from, and adapt to climate and land use change (that is, communities that have higher SVIs). When a 10-year or extreme high flow occurs, more vulnerable communities are likely to be more negatively impacted than less vulnerable communities (Finch and others 2010; Cutts and others 2018). We identified where estimates for each subbasin and each future scenario would lie in a 2D risk matrix based on *x* and *y* axes coordinates and used the quadrant where subbasin SWAT and SVI pairs fell when mapping these results spatially (Figure S2c). We used the same approach as discussed previously for SWAT results to summarize high-risk SWAT and SVI results across the four future scenarios. More specifically, we generated Figure 4C from the high-risk results presented in Figure S6 and generated Figure 4E from the high-risk results presented in Figure S7. Similar to the SVI results approach, we used both subbasin (low-resolution) and census tract (high-resolution) scales to account for spatial heterogeneity in social vulnerability. See ''Social Vulnerability'' section for further discussion on why we included both scales in our analysis.

Data Analysis and Availability

We analyzed these data using ArcGIS (version 10.4.1; ESRI 2011), Python (version 2.7; Python Software Foundation 2010), and R (version 3.4.3; R Core Team 2017). All data and scripts associated with this publication are available on GitHub at https://github.com/sheilasaia/paper-yadkin-swat-svi-study and Zenodo (DOI: http://www.doi.org/10.5281/zenodo.2635878).

Results

Streamflow

PC_{10} and PC_{ext} values were largely positive throughout the YPD (Figure 3). Additionally, there was greater variation in PC_{10} compared to PC_{ext} values between the four future scenarios. Variation in PC_{10} values showed no clear trend toward the watershed outlet (Figure 3A), but with the exception of a few subbasins (for example, 18, 21, 22, and 25), the variation in PC_{ext} values tended to increase toward the watershed outlet (Figure 3B). The range of both PC_{10} and PC_{ext} values tended to shift upward toward the watershed outlet. For

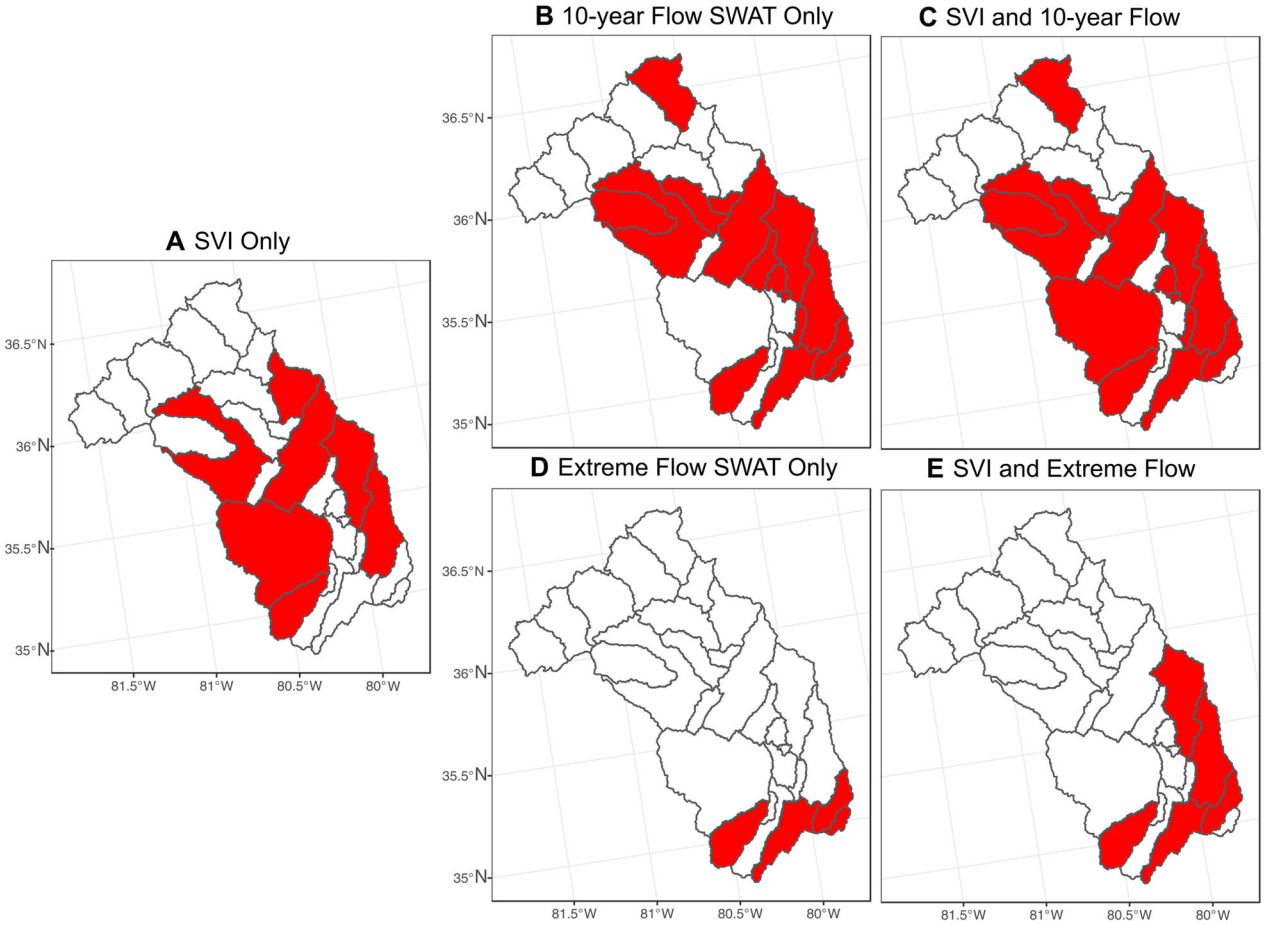

Figure 4. Comparison of high-risk subbasins in the Yadkin–Pee Dee River Watershed summarized for all four future scenarios considering **A** Social Vulnerability Index (SVI) results, Soil Water Assessment Tool (SWAT) results for **B** 10-year and **C** extreme high flows, and the spatial intersection of SVI and SWAT results for **D** 10-year and **E** extreme high flows using the risk matrix. Tabulated results are included in Tables S3–S5. Low- and medium-risk categories and results from all four future scenarios are included in the supplemental material (Figures S3–S7) (Color figure online).

example, we calculated a PC_{10} of 0–23.8% for subbasin 5 near the headwaters and 16.2–57.1% for subbasin 28 near the outlet, depending on the future scenario. We calculated a PC_{ext} of 2.2–6.2% for subbasin 5 near the headwaters and 14.6–59.5% for subbasin 28 near the outlet, depending on the future scenario. Looking at the number of days per year where streamflow was $\geq F_{10}$ or $\geq F_{ext}$, there was larger variation in the projected period compared to the baseline period for both 10-year and extreme flows (Figure S8). Additionally, the number of days per year where projected streamflow was $\geq F_{10}$ tended to increase more toward the watershed outlet (Figure S8b) compared to that for extreme flows (Figure S8d). For extreme high flows, the number of days per year where projected streamflow $\geq F_{ext}$ did not show as dramatic an increase toward the watershed outlet compared to 10-year high flows.

After summarizing the four future scenarios for 10-year high flows (Figure S3), there were 16 unique high-risk subbasins based on PC_{10} from SWAT results (Table S3, Figure 4B). PC_{10} for these 16 subbasins ranged from 54.8% (subbasin 23) to 133.3% (subbasin 18). Six of the 16 showed pronounced increases in streamflow for at least half of the future scenarios. For example, subbasin 14 showed ≥ 50% increase in PC_{10} for CSIRO 4.5 and CSIRO 8.5 future scenarios and subbasin 18 showed ≥ 50% increase in PC_{10} for CSIRO 4.5, CSIRO 8.5, and MIROC 8.5 future scenarios. We identified no subbasins in the high-risk class for all four future scenarios. After summarizing the four future scenarios for extreme high flows (Figure S4), we identified four unique high-risk sub-

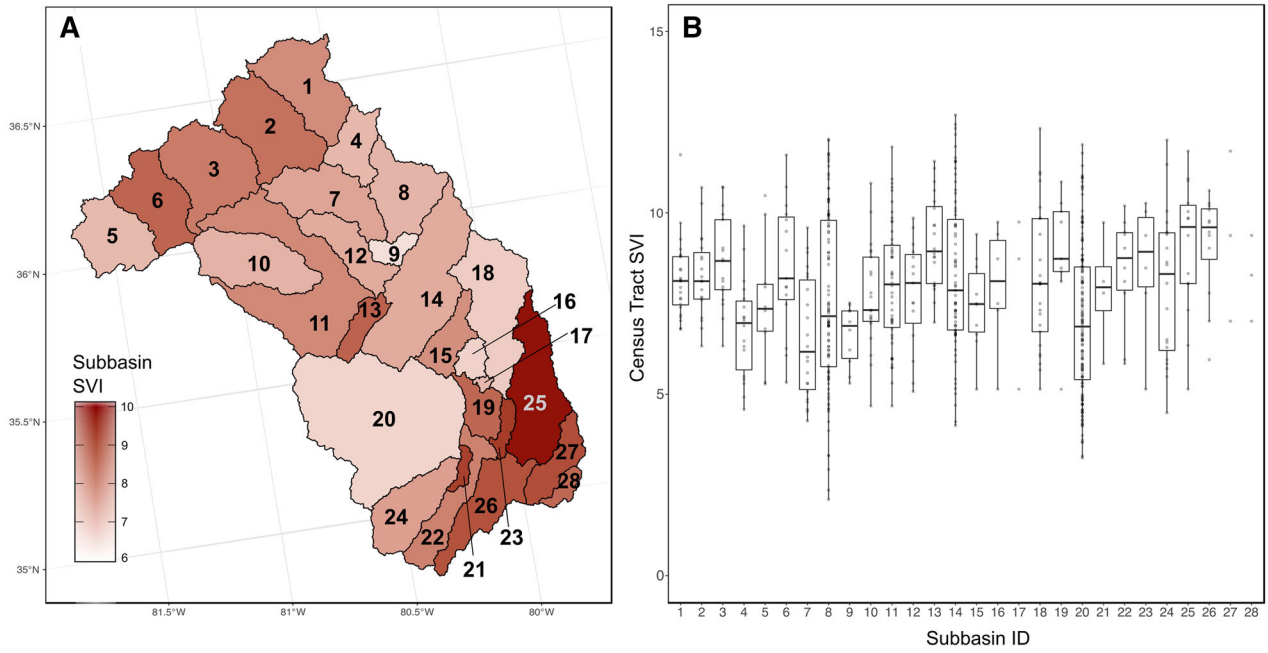

Figure 5. **A** Subbasin Social Vulnerability Index (SVI) results for the Yadkin–Pee Dee River Watershed (YPD) calculated as the area weighted average of census tract SVIs within each subbasin. **B** Census tract SVIs in each YPD subbasin (corresponding subbasin IDs are labeled in **A**). Box and whiskers are omitted for subbasins 17, 27, and 28 because there were $n = 3$ census tracts. Note subbasin SVI scale ranges from 6 to 10 (Color figure online).

basins based on PC_{ext} from SWAT results (Table S3, Figure 4D). All four of these subbasins were also identified based on PC_{10} from SWAT results. In these four subbasins, PC_{ext} ranged from 51.6% (subbasin 27) to 59.5% (subbasin 28) and half (subbasins 27 and 28) had a pronounced (≥ 50%) increase in streamflow response in two or more future scenarios. Three of the 16 high-risk subbasins had a > 100% increase in 10-year flows between the baseline and projection datasets. We discuss the integration of SWAT and SVI results using the risk matrix (that is, Figure 4C, E) in ''Comparison of Approaches'' section.

Social Vulnerability

Social vulnerability varied across the YPD at census track and subbasin scales (Figures 5 and S9). The minimum, mean, and maximum census tract SVIs for the YPD were 2.1, 7.8, and 12.7, respectively. For comparison, the minimum, mean, and maximum census tract SVIs for the continental USA were 0.09, 7.3, and 13.7, respectively. The first standard deviation of all census tract SVIs in the YPD and continental USA datasets were similar: 2.1 and 2.2, respectively. According to two-sided Kolmogorov–Smirnov tests, the distribution of NC and YPD census tract SVIs was significantly different and shifted to the right compared the distribution of US census tract SVIs (Figure S10; $p < 0.05$). However, the distribution of NC and YPD census tract SVIs is not significantly different (Figure S10; $p = 0.58$). At the subbasin scale, the minimum, mean, and maximum subbasin SVIs for the YPD were 6.5, 7.9, and 9.9, respectively. The first standard deviation of all subbasin SVIs for the YPD was 0.9. See ''Social Vulnerability'' section for further discussion on how and why we incorporated both the census tract and subbasin SVI results into our analysis.

There were seven unique high-risk subbasins based on SVI results (Table S4, Figures 4A and S5). One subbasin (subbasin 25) had a subbasin SVI that was > 9.6 (that is, first standard deviation of all continental USA census tract SVIs) and the remaining six subbasins had at least one census tract with a census tract SVI that was > 11.8 (that is, second standard deviation of all continental USA census tract SVIs). Five of the seven high-risk subbasins had subbasin SVIs > 7.3 (that is, mean of all continental USA census tract SVIs). Several of these seven subbasins had large ranges in census tract SVIs (Figure 5B). For example, subbasin 8 had the largest range in census tract SVIs; its minimum census tract SVI was 2.1 and its maximum census

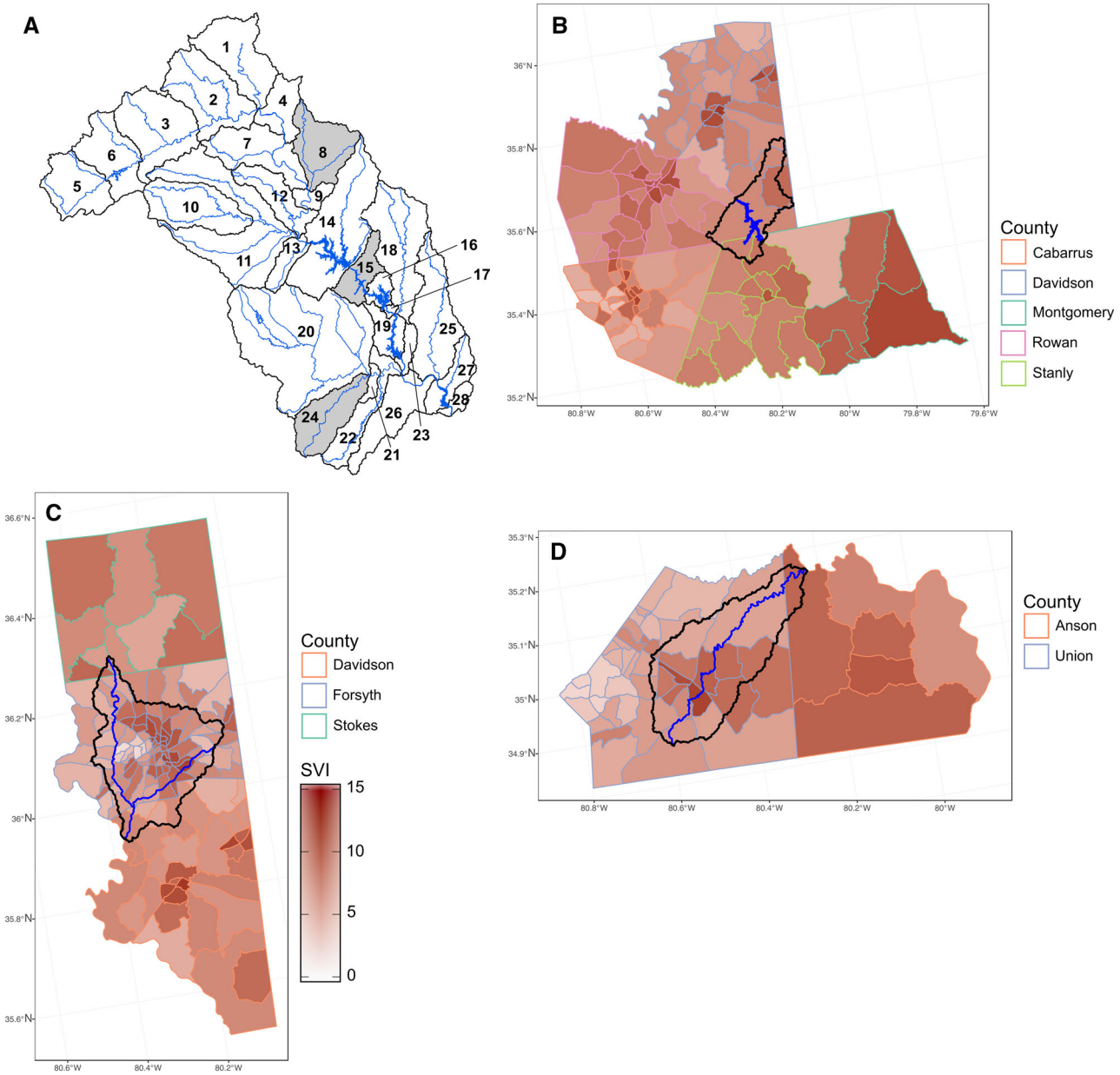

Figure 6. **A** Watershed view of (**B**–**D**) subbasins highlighted in *Comparison of Approaches*: **B** subbasin 15, **C** subbasin 8, and **D** subbasin 24. Black and blue lines represent subbasin boundaries and the Yadkin–Pee Dee River, respectively. Census tract boundary outlines are colored by county, and background shading represents census tract Social Vulnerability Index (SVI) (Color figure oline).

tract SVI was 12.0. Based on CDFs for each of these seven subbasins, anywhere from < 5 to 75% of the subbasin area contained communities classified as high-risk based on a census tract SVIs > 9.6 (Figure S11). For example, approximately 25% of the area of subbasin 8 and 75% of the area of subbasin 25 included census tracts SVIs > 9.6. Besides the high-risk subbasins, there were 18 medium-risk subbasins and three low-risk subbasins (Figure S5). We discuss the integration of SWAT and SVI results using the risk matrix (that is, Figure 4C, E) in ''Comparison of Approaches'' section.

Discussion

Streamflow

Our results suggest a future with increased frequency of 10-year and extreme flows, which is consistent with and exacerbated by the projected conversion of forested lands to developed and

agricultural lands in the YPD (Figure S12). As a consequence of these changes, more surface runoff is expected to be transported to streams via impervious and cultivated surfaces (Ogden and others 2011; Suttles and others 2018). Over half the subbasins exhibited > 50% increase in PC_{10} and one-seventh of the subbasins showed > 50% increase PC_{ext}. Based on SWAT results, over 35% of the high-risk subbasins were indicated as such by at least half the future scenarios (that is, three-eighths of subbasins for PC_{10} and half of subbasins for PC_{ext}; Table S3). Therefore, across the envelope of future climate and land use changes, it is likely that streamflow in the YPD will exhibit more frequent 10-year and extreme high flows. Based on previous studies, the impacts of climate and land use change on future streamflow were additive in the YPD (Suttles and others 2018). Additionally, in select subbasins such as subbasin 18 (that is, Uwharrie River Watershed), future land use change had a larger impact on streamflow than climate change where land was converted from forested to urban (Martin and others 2017).

In this study, the Hadley 4.5 scenario projected the largest increase in average annual temperature and smallest increase in average annual precipitation compared to the other future scenarios (Table 2). This translates into drier average (that is, lowest number of 10-year flows exceedances in the projection dataset; Figure S8b) and wetter extreme (that is, highest number of extreme flow exceedances the projection dataset; Figure S8d) streamflow conditions in the YPD. Additionally, the CSIRO 4.5 scenario projects the smallest increases in average annual temperature and the largest increase in average annual precipitation compared to the other future scenarios (Table 2), which translates to the wettest average and moderately extreme streamflow conditions in the YPD. These results are consistent with findings that the Hadley and CISRO GCMs tend to projects higher future precipitation totals in the SEUS compared to the MIROC GCM (Steinschneider and others 2015). We note that this analysis examines mid-twenty-first century changes. Since future climate scenarios tend to diverge more rapidly in the late-twenty-first century (IPCC 2014), analysis of this later period will likely yield wider response ranges than presented here. Further, we note that projected daily streamflow may be conservative since backcast baseline GCM results under predicted observed annual average and 90th percentile flows (Table S2, Figure S1).

Social Vulnerability

Scaling census tract SVI results to the subbasin scale, which was necessary to make comparisons with SWAT results and facilitate water resources management at the watershed scale, reduced SVI heterogeneity across the YPD. Namely, we observed that the first standard deviation of subbasin SVIs for the YPD was smaller than the first standard deviation of census tract SVIs (0.9 compared to 2.1, respectively). We are not aware of any studies that have tested whether a risk matrix framework can adequately account for discrepancies in scale between social vulnerability and hydrologic model results. Therefore, we used both overall subbasin (low-resolution) and census tract (high-resolution) SVI results to classify subbasins because we wanted to account for (1) scale discrepancies between watershed and demographic (that is, census tract) boundaries and (2) socioeconomic disparities between communities in the same subbasin. We also found that some subbasins contained wide ranges in social vulnerability, which suggests that some communities within the subbasin may be more able to adapt to future climate and land use change than others. This result further justifies the importance of simultaneously considering different scales of SVI results.

Our results also suggest that NC and YPD census tracts are more socially vulnerable compared to census tracts at the national (US) scale. Furthermore, socially vulnerable communities in the YPD can be found in both urban and rural settings. Approximately 45% of the area of subbasin 8, which contains the city of Winston-Salem, NC, is made up of census tracts with SVIs > 7.3 (that is, the mean of all census tract SVIs in the continental USA) and 25% of the area is made up of census tracts with SVI > 9.6 (that is, first standard deviation of all census tract SVIs in the continental USA; Figure S11). For urban communities in the SEUS, increases in high streamflow events due to climate and land use change may lead to increases in economic vulnerabilities such as loss of property, and like rural communities, increases in health vulnerabilities (Carter and others 2018). With respect to rural communities in the SEUS, increases in high streamflow events due to climate and land use change may lead to economic vulnerabilities such as reduction in labor hours and loss of profit due to crop loss and health vulnerabilities such as increases in exposure to extreme events and new local diseases (Carter and others 2018). In contrast to the urban communities in subbasin 8, subbasin 25 had the highest subbasin SVI in the YPD and

contained the rural communities of Troy, NC and Biscoe, NC. Approximately 90% of its area was made up of census tracts with SVIs > 7.3 and 75% of its area is made up of census tracts SVIs > 9.6 (Figure S11). These results highlight the importance of considering both urban and rural communities while developing climate change adaptation plans.

Comparison of Approaches

The goal of this study was to assess how combining SWAT and SVI results using a risk matrix effects the spatial distribution of climate change adaptation planning compared to using SWAT and SVI results alone. To answer our research question, we compared the spatial distribution of high-risk subbasins based on: (1) SWAT results, (2) SVI results, and (3) the integration of SWAT and SVI results using a risk matrix. We summarize general spatial patterns and highlight three high-risk subbasins for each of the three approaches (that is, SWAT results, SVI results, and SWAT and SVI results). More specifically, we discuss the Yadkin River (subbasin 15), Muddy Creek (subbasin 8), and Richardson Creek (subbasin 24) subbasins.

Based on SWAT results, the 16 subbasins with the largest projected increases in 10-year high flows were located in middle to lower parts of the YPD. The four subbasins with the largest increase in extreme high flows overlapped with these 10-year high flow subbasins and were located in lower parts of the YPD (Figure 4B, D). Subbasin 1, located in the headwaters of the YPD, is an exception to this general spatial pattern. It was indicated as high-risk in the CSIRO 4.5 future scenario based on SWAT results (Table S3, Figure S3c) likely because of projected increases in developed and agricultural land uses and projected decreases in forested land use within the subbasin (Figure S12). We selected Yadkin River (subbasin 15) as a SWAT results example because it represents a subbasin that might be selected for climate change adaptation planning if only biophysical factors were considered (Figure 6B). Subbasin 15 is located in the middle of the YPD along the main stem of the Yadkin River and contains the towns of Denton, NC, Misenheimer, NC, and Richfield, NC. The low density of census tracts within subbasin 15 suggests that these communities are rural; people are likely to live farther apart (Figure 6B). For the CSIRO 4.5 future scenario, subbasin 15 was projected to have a 64.5% increase in 10-year and extreme high flows (Table S3). This increase in the number of 10-year and extreme high flows is likely due to the conversion of forested land uses to developed land (Figure S12). More specifically, subbasin 15 consisted of primarily forested (70%) lands at baseline conditions while future scenarios project that developed lands will increase over 14 times. However, although subbasin 15 was classified as high-risk based on SWAT results, it may have a greater socioeconomic capacity to adapt to future climate and land use change impacts on streamflow compared to other subbasins in the YPD. Namely, its subbasin SVI (that is, 7.9) was within the first standard deviation of census tract SVIs for the USA (that is, 9.6) and all of its area contained census tract SVIs < 9.6 (Figure S11).

Based on SVI results, the seven most vulnerable subbasins were located further away from the mainstem of the Yadkin–Pee Dee River and consisted of both urban and rural socially vulnerable communities at the census tract scale (Figure 4A). Additionally, we observed spatially heterogeneous census tract SVIs throughout the YPD; several subbasins (for example, subbasins 8, 14, and 20 in Figure 5B) showed large ranges in census tract SVIs indicating socioeconomic disparities between communities within the same subbasin and associated spatially uneven impacts of environmental hazards (Finch and others 2010; Cutts and others 2018; Hale and others 2018). We selected Muddy Creek (subbasin 8) as a SVI results example because it represents a subbasin that might be selected for climate change adaptation planning if only socioeconomic factors were considered (Figure 6C). Subbasin 8 contains the city of Winston-Salem, NC, and is one of the most highly populated subbasins within the YPD given that it has a high density of census tracts (Figure 6C) and large (34%) percentage of developed land use. Subbasin 8 is part of Forsyth County which is projected to experience population growth by 2060 (USFS 2012; Wear and others 2013). As discussed previously, approximately 25% of the area of subbasin 8 was made up of census tracts that had a census tract SVI > 9.6 (that is, first standard deviation of all census tract SVIs in the continental USA). Especially vulnerable communities are located on the northeastern, eastern, and southeastern sides of the city between the western and eastern forks of the Muddy Creek; some especially vulnerable communities overlap with the eastern fork of the Muddy Creek (Figure 6C). However, although subbasin 8 was classified as high-risk based on SVI results, it will experience more limited (< 25% increase) either 10-year or extreme high flows under any future scenario compared to other subbasins in the YPD (Figures S3 and S4).

In combining SWAT and SVI results, the 14 most vulnerable subbasins were mainly located in the middle and lower parts of the YPD (Figure 4C, E). The majority of these 14 subbasins showed agreement among two or more future scenarios for both 10-year and extreme high flows (Table S5, Figures S6, S7, and S13). Of these 14 subbasins, subbasin 25 falls into the upper-left-most corner of the risk matrix used in this study based on its large PC_{10} and subbasin SVI, whereas the remaining subbasins fall into this region of the risk matrix used in this study based on large PC_{10} and maximum census tract SVI. For these 14 subbasins, about 1–75% of their area was composed of census tracts with census tract SVIs > 9.6 (that is, first standard deviation of all census tract SVIs in the continental USA; Figure S11). Thus, these 14 subbasins are both socially vulnerable and expected to have large increases in 10-year and extreme high flows.

We selected Richardson Creek (subbasin 24) as a SVI and SWAT example because it represents a subbasin that was identified as high-risk based on both SVI and SWAT results using the risk matrix used in this study (Figure 6D). Subbasin 24 contains the town of Monroe, NC, and is located within Union County, which is projected to experience population growth by 2060 (USFS 2012; Wear and others 2013). In terms of socioeconomic factors, subbasin 24 has a subbasin SVI of 7.6 which is > 7.3 (that is, mean of all census tract SVIs in the continental USA) and about 20% of its area is composed of census tracts with census tract SVIs > 9.6 (Figure S11). Especially vulnerable communities are located in the middle of the subbasin—with the most vulnerable being located right along Richardson Creek (Figure 6D). In terms of biophysical factors, subbasin 24 is projected to have > 50% increases in 10-year and extreme high flows in half of the future scenarios (Table S5); this is likely due to projected increases in developed land (Figure S12). More specifically, at baseline conditions subbasin 24 consisted of 41.4% forested, 32.3% non-stocked, 19.7% agriculture, 5.9% developed (the remainder is wetlands and water) land uses. Based on land use projections for subbasin 24, developed land will increase almost six times and agricultural land will nearly double as forested lands are lost (Figure S12). Thus, by using a risk matrix to integrate SWAT and SVI results, we can identify subbasins where projected increases in streamflow overlap with vulnerable communities.

Future Directions

In this study, we used SWAT to simulate the combined impact of land use and climate change on streamflow because these biophysical influences will likely occur together. We also combined these biophysical influences because previous research in the YPD focused on the contributions of each to changes in streamflow (that is, Martin and others 2017; Suttles and others 2018); thus, our study extends previous work to include socioeconomic factors. However, opportunities exist to explore the relative impacts and interactions of climate and land use change on social vulnerability with respect to future low and high streamflow events.

Addressing scaling discrepancies between water resources management at the watershed and subbasin scale with decision making at the census tract or county scale is an ongoing and understudied issue (Molle 2009; Gober and others 2013). We attempted to address this by including both subbasin and census tract scale SVI results when applying a risk matrix. However, opportunities exist to refine the methods presented here for the purpose of addressing the impacts of future climate and land use change on streamflow on across county, state, and country boundaries. In addition to exploring different approaches for SVI scaling, social vulnerability in YPD communities may change and we are not aware of datasets that project SVI. Therefore, future work may use longitudinal methods (for example, Cutter and Finch 2008 and Cutts and others 2018) to identify historic trends in social vulnerability that can be used to inform future climate change adaptation planning and engage local communities.

We emphasize that the integrated SVI and SWAT results be used as an initial step to inform climate change adaptation planning. Further, recent publications agree that census data should be used as a screening tool to highlight (or triage) areas for further scrutiny (Emanuel 2018). Feedback from community members is a key component of effective water resources management research (Sivapalan and others 2012; Gober and Wheater 2015; Srinivasan and others 2017; Cutts and others 2018) as is the realization that technical solutions to future climate and land use change are more likely to be effective with community support (Schirmer and Dyer 2018). SVI results are publicly available for the continental USA (see https://svi.cdc.gov/S

VIDataToolsDownload.html), and SWAT studies have been established across the USA and around the world; therefore, there is an opportunity extend the methods used in this study to other regions of the USA and abroad to help vulnerable communities adapt to climate and land use change induced impacts on water resources.

Conclusions

This study compared the spatial distribution of high-risk subbasins in the Yadkin–Pee Dee River Watershed (YPD) in North Carolina, USA, based on three approaches: (1) percent increase in Soil and Water Assessment Tool (SWAT) simulated 10-year and extreme high flows between baseline (1982–2002) and projected (2050–2070) periods due to climate and land use change, (2) the degree of community vulnerability according to a Social Vulnerability Index (SVI), and (3) the integration of SWAT and SVI results using a risk matrix. We showed how climate change adaptation planning that relies on either the first (that is, SWAT results) or second (that is, SVI results) approaches may miss locations where future increases in streamflow overlap with vulnerable communities. Further, we demonstrated how the third approach (that is, SWAT and SVI results) considers both biophysical and socioeconomic factors by identifying high-risk subbasins that are projected to experience increases in 10-year and extreme high flows and that also contain vulnerable communities with limited capacity to adapt to these future increases in streamflow due to climate and land use change. For 10-year high flows, we identified high-risk subbasins in the middle and lower parts of the YPD where multiple climate–land use change scenarios projected increases in future 10-year flows and had either a large (low-resolution) subbasin SVI or contained census tracts with large (high-resolution) census tract SVIs. For extreme high flows, all high-risk subbasins were located in the lower parts of the YPD and overlapped with subbasins previously identified under the 10-year high flow case. In summary, combining SWAT and SVI results using a risk matrix can be used to extend the use of these results on their own by providing the first step (that is, identifying spatial units—either census tracts or subbasins) of a multi-step process in climate change adaptation planning. Besides describing spatial patterns in risk, SWAT results suggest that future 10-year and extreme flows are likely to be more frequent and variable in the YPD. We identified vulnerable communities throughout the YPD. We identified several subbasins with large ranges in census tract SVIs, which suggests there are socioeconomic disparities between communities within these subbasins. In this study, we used the YPD as an example and suggest the risk matrix approach can be applied to other regions where baseline streamflow, projected streamflow, and SVI results are available.

Acknowledgements

SMS and KMS were supported by an appointment to the United States Department of Agriculture Forest Service (USFS) Research Participation Program administered by the Oak Ridge Institute for Science and Education (ORISE) through an interagency agreement between the United States Department of Energy (DOE) and the USFS. ORISE is managed by Oak Ridge Associated Universities (ORAU) under DOE contract number DE-SC0014664. All opinions expressed in this paper are the authors' and do not necessarily reflect the policies and views of USFS. The manuscript was greatly improved by reviews from two anonymous reviewers, Dr. Louis Iverson and Dr. Travis Warzineak. All data and scripts associated with this publication are available on GitHub at https://github.com/sheilasaia/paper-yadkin-swat-svi-study and Zenodo (DOI: http://www.doi.org/10.5281/zenodo.2635878).

References

Ahiablame L, Sinha T, Paul M, Ji JH, Rajib A. 2017. Streamflow response to potential land use and climate changes in the James River watershed, Upper Midwest United States. J Hydrol Reg Stud 14:150–66.

Arnold JG, Srinivasan R, Muttiah RS, Williams JR. 1998. Large area hydrologic modeling and assessment part 1: model development. J Am Water Res Assoc 34:73–89.

Carter LM, Jones JW, Berry L, Burkett V, Murley JF, Obeysekera J, and others. 2014. Chapter 17: Southeast and the Caribbean. In: Melillo JM, Richmond TC, Yohe GW, Eds. Climate Change Impacts in the United States: The Third National Climate Assessment. Washington, DC: U.S. Global Change Research Program. pp 396–417.

Carter LM, Terando A, Dow K, Hiers K, Kunkel KE, Lascurain A, and others. 2018. Chapter 19: Southeast. In: Reidmiller DR, Avery CW, Easterling DR, Kunkel KE, Lewis KLM, Maycock TK, Stewart BC, Eds. Impacts, risks, and adaptation in the United States: Fourth National Climate Assessment. Washington, DC: U.S. Global Change Research Program. pp 743–808.

Cutter SL, Boruff BJ, Shirley WL. 2003. Social vulnerability to environmental hazards. Soc Sci Q 84:242–61.

Cutter SL, Finch C. 2008. Temporal and spatial changes in social vulnerability to natural hazards. Proc Natl Acad Sci USA 105:2301–6.

Cutts BB, Greenlee AJ, Prochaska NK, Chantrill CV, Contractor AB, Wilhoit JM, Abts N, Hornik K. 2018. Is a clean river fun for all? Recognizing social vulnerability in watershed plan-

ning. PLoS ONE 13:e0196416. https://doi.org/10.1371/journal.pone.0196416.

Emanuel RE. 2018. Flawed environmental justice analyses. Science 357:260.

Emrich CT, Cutter SL. 2011. Social vulnerability to climate-sensitive hazards in the Southern United States. Weather Clim Soc 3:193–208.

ESRI. 2011. ArcGIS desktop: release 10. Redlands: Environmental Systems Research Institute.

Fekete BM, Vörösmarty CJ, Roads JO, Willmott CJ. 2004. Uncertainties in precipitation and their impacts on runoff estimates. J Clim 17:294–304.

Federal Emergency Management Agency (FEMA). 2018. Guidance for flood risk analysis and mapping: accepting numerical models for use in the NFIP. Guidance Document 98. p 12.

Ficklin DL, Abatzoglou JT, Robeson SM, Null SE, Knouft JH. 2018. Natural and managed watersheds show similar responses to recent climate change. Proc Natl Acad Sci 115:8553–7.

Finch C, Emrich CT, Cutter SL. 2010. Disaster disparities and differential recovery in New Orleans. Popul Environ 31:179–202.

Flanagan BE, Gregory EW, Hallisey EJ, Heitgerd JL, Lewis B. 2011. A Social Vulnerability Index for disaster management. J Homel Secur Emerg Manag 8:3.

Francesconi W, Srinivasan R, Pérez-Miñana E, Willcock SP, Quintero M. 2016. Using the soil and water assessment tool (SWAT) to model ecosystem services: a systematic review. J Hydrol 535:625–36.

Gassman PW, Reyes MR, Green CH, Arnold JG. 2007. The soil and water assessment tool: historical development, applications, and future research directions. Trans ASABE 50:1211–50.

Gober P, Larson KL, Quay R, Polsky C, Chang H, Shandas V. 2013. Why land planners and water managers don't talk to one another and why they should!. Soc Nat Resour 26:356–62.

Gober P, Wheater HS. 2015. Debates—perspectives on socio-hydrology: modeling flood risk as a public policy problem. Water Resour Res 51:4782–8.

Guillard-Gonçalves C, Cutter SL, Emrich CT, Zêzere JL. 2015. Application of Social Vulnerability Index (SoVI) and delineation of natural risk zones in Greater Lisbon, Portugal. J Risk Res 18:651–74.

Hale RL, Flint CG, Jackson-Smith D, Endter-Wada J. 2018. Social dimensions of urban flood experience, exposure, and concern. J Am Water Resour Assoc 54:1–14.

Hamel P, Daly E, Fletcher TD. 2013. Source-control stormwater management for mitigating the impacts of urbanisation on baseflow: a review. J Hydrol 485:201–11.

Hayhoe K, Wuebbles DJ, Easterling DR, Fahey DW, Doherty S, Kossin J, and others. 2018. Chapter 2: Our Changing Climate. In: Reidmiller DR, Avery CW, Easterling DR, Kunkel KE, Lewis KLM, Maycock TK, Stewart BC, Eds. Impacts, risks, and adaptation in the United States: Fourth National Climate Assessment. Washington, DC: United States Global Research Program. pp 72–144.

Hovenga PA, Wang D, Medeiros SC, Hagen SC, Alizad K. 2016. The response of runoff and sediment loading in the Apalachicola River, Florida to climate and land use land cover change. Earth's Future 4:124–42.

Hsiang SM, Kopp R, Jina A, Rising J, Delgado M, Mohan S, Rasmussen DJ, Muir-Wood R, Wilson P, Oppenheimer M, Larsen K, Houser T. 2017. Estimating economic damage from climate change in the United States. Science 356:1362–9.

Interagency Advisory Committee on Water Data (IACWD). 1982. Flood flow frequency: United States Geological Survey, Interagency Advisory Committee on Water Data, bulletin 17B of the hydrology subcommittee. Reston: United States Department of the Interior. p 194.

International Panel on Climate Change (IPCC). 2014. Climate Change 2014: synthesis report. In: Core Writing Team, Pachauri RK, Meyer LA, Eds. Contribution of working groups I, II and III to the Fifth Assessment Report of the Intergovernmental Panel on Climate Change. Geneva: IPCC. p 151.

Iverson LR, Matthews SN, Prasad AM, Peters MP, Yohe G. 2012. Development of risk matrices for evaluating climatic change responses of forested habitats. Clim Change 114:231–43.

Kc B, Shepherd JM, Gaither CJ. 2015. Climate change vulnerability assessment in Georgia. Appl Geogr 62:62–74.

Kim Y, Band LE, Song C. 2014. The influence of forest regrowth on the stream discharge in the North Carolina Piedmont watersheds. J Am Water Resour Assoc 50:57–73.

Krysanova V, Srinivasan R. 2014. Assessment of climate and land use change impacts with SWAT. Reg Environ Change 15:431–4.

Kunkel KE, Stevens LE, Stevens SE, Sun L. 2013. Regional climate trends and scenarios for the U.S. National Climate Assessment. Part 2. Climate of the Southeast U.S. NOAA Technical Report NESDIS 142-2. Washington, DC. p 103.

Laseter SH, Ford CR, Vose JM, Swift LW. 2012. Long-term temperature and precipitation trends at the Coweeta Hydrologic Laboratory, Otto, North Carolina, USA. Hydrol Res 43:890.

Lee KS, Chung E-S. 2007. Hydrological effects of climate change, groundwater withdrawal, and land use in a small Korean watershed. Hydrol Process 21:3046–56.

Ma X, Xu J, van Noordwijk M. 2010. Sensitivity of streamflow from a Himalayan catchment to plausible changes in land cover and climate. Hydrol Process 24:1379–90.

Major DC, O'Grady M. 2010. Appendix B, adaptation assessment guidebook: New York City Panel on Climate Change. Ann N Y Acad Sci 1196:229–92.

Martin KL, Hwang T, Vose JM, Coulston JW, Wear DN, Miles B, Band LE. 2017. Watershed impacts of climate and land use changes depend on magnitude and land use context. Ecohydrology 10:1–17.

McNulty S, Meyers JM, Caldwell P, Sun G. 2013. Chapter 3: climate change summary. In: Wear DN, Greis JG, Eds. The southern forest futures project: technical report. Ashville, NC: United States Department of Agricultural Forest Service Research and Development Southern Research Station. General technical report SRS-179. pp 27–43.

Molle F. 2009. River-basin planning and management: the social life of a concept. Geoforum 40:484–94.

Moriasi DN, Arnold JG, Van Liew MW, Bingner RL, Harmel RD, Veith TL. 2007. Model evaluation guidelines for systematic quantification of accuracy in watershed simulations. Trans Am Soc Agric Biol Eng 50:885–900.

Natkhin M, Dietrich O, Schäfer MP, Lischeid G. 2015. The effects of climate and changing land use on the discharge regime of a small catchment in Tanzania. Reg Environ Change 15:1269–80.

Neitsch SL, Arnold JG, Kiniry JR, Williams JR. 2011. Soil and water assessment tool theoretical documentation. Texas Water Resources Institute technical report no. 406. Temple, TX. p 647.

North Carolina Department of Transportation (NCDOT). 2012. North Carolina Municipal Boundary. NC OneMap, 1 Nov. 2012, http://data.nconemap.gov. NC OneMap is an initiative of the North Carolina Geographic Information Coordinating Council http://it.nc.gov/gicc.

O'Gorman PA, Schneider T. 2009. Scaling of precipitation extremes over a wide range of climates simulated with an idealized GCM. J Clim 22:5676–85.

Ogden FL, Raj Pradhan N, Downer CW, Zahner JA. 2011. Relative importance of impervious area, drainage density, width function, and subsurface storm drainage on flood runoff from an urbanized catchment. Water Resour Res 47:W12503.

Ojima D, Iverson LR, Sohngen BL, Vose JM, Woodall CW, Domke GM, Peterson DL, Littell JS, Matthews SN, Prasad AM, Peters MP, Yohe GW, Friggens MM. 2014. Chapter 9: Risk Assessment. In: Peterson DL, Vose JM, Patel-Weynand T, Eds. Climate change and United States Forests. Dordrecht: Springer. p 261.

Python Software Foundation. 2010. Python language reference, version 2.7. Available at http://www.python.org/.

R Core Team. 2017. R: A language and environment for statistical computing. Vienna: R Foundation for Statistical Computing. URL: https://www.R-project.org/.

Raiffa H, Schlaiffer R. 2000. Applied statistical decision theory. New York: Wiley Classics. p 356p.

Quist J, Vergragt P. 2006. Past and future of backcasting: the shift to stakeholder participation and a proposal for a methodological framework. Futures 38:1027–45.

Schirmer J, Dyer F. 2018. A framework to diagnose factors influencing proenvironmental behaviors in water-sensitive urban design. Proc Natl Acad Sci 115:E7690–9.

Schwartz HG. 2010. Adaptation and the impacts of climate change on transportation. The bridge: linking engineering and society. Natl Acad Eng 40:5–13.

Schwartz, HG, Meyer M, Burbank CJ, Kuby M, Oster C, Posey J, Russo EJ, Rypinski A. 2014: Chapter 5: transportation. In: Melillo JM, Richmond TC, Yohe GW, Eds. Climate change impacts in the United States: the third national climate assessment. Washington, DC: U.S. Global Change Research Program. pp 130–149.

Sivapalan M, Savenije HHG, Blöschl G. 2012. Socio-hydrology: a new science of people and water. Hydrol Process 26:1270–6.

Srinivasan V, Sanderson M, Garcia M, Konar M, Blöschl G, Sivapalan M. 2017. Prediction in a socio-hydrological world. Hydrol Sci J 62:338–45.

Steinschneider S, McCrary R, Mearns LO, Brown C. 2015. The effects of climate model similarity on probabilistic climate projections and the implications for local, risk-based adaptation planning. Geophys Res Lett 42:5014–22.

Suttles KM. 2017. Assessment of watershed vulnerability to land use and climate change. North Carolina State University, Master's thesis.

Suttles KM, Singh NK, Vose JM, Martin KL, Emanuel RE, Coulston JW, Saia SM, Crump MT. 2018. Assessment of hydrologic vulnerability to urbanization and climate change in a rapidly changing watershed in the Southeast U.S. Sci Total Environ 645:806–16.

Terando AJ, Costanza J, Belyea C, Dunn RR, McKerrow A, Collazo JA. 2014. The southern megalopolis: using the past to predict the future of urban sprawl in the Southeast U.S. PLoS ONE 9:e102261.

United States Census Bureau (USCB). 2008. A compass for understanding and using American community survey data: what general data users need to know. Washington, DC: United States Government Printing Office. p 68.

United States Environmental Protection Agency (USEPA). 2009. Technical guidance on implementing the stormwater runoff requirements for federal projects under section 438 of the energy independence and security act. USEPA report 841-B-09-001. Washington, DC: Office of Water. p 63.

United States Department of Agriculture Forest Service (USFS). 2012. Future scenarios: a technical document supporting the Forest Service 2010 RPA Assessment. General technical report RMRS-GTR-272. USFS, Rocky Mountain Research Station, Fort Collins, CO. p 34.

Van der Voorn T, Pahl-Wostl C, Quist J. 2012. Combining backcasting and adaptive management for climate adaptation in coastal regions: a methodology and a South African case study. Futures 44:346–64.

Vogelmann JE, Howard SM, Yang L, Larson CR, Wylie BK, Van Driel JN. 2001. Completion of the 1990's national land cover data set for the conterminous United States. Photogramm Eng Remote Sensing 67:650–62.

Walsh J, Wuebbles D, Hayhoe K, Kossin J, Kunkel K, Stephens G, and others. 2014. Ch. 2: our changing climate. In: Melillo JM, Richmond TC, Yohe GW, Eds. Climate Change Impacts in the United States: the third national climate assessment. Washington, DC: United States Global Change Research Program. pp 19–67.

Wear, DN. 2013. Chapter 4: forecasts of land uses. In: Wear DN, Greis JG, Eds. The southern forest futures project: technical report. General technical report SRS-179. Ashville, NC: United States Department of Agricultural Forest Service Research and Development, Southern Research Station. pp 45–71.

Wear DN, Huggett R, Greis JG. 2013. Chapter 2: constructing alternative futures. In: Wear DN, Greis JG, Eds. The southern forest futures project: technical report. General technical report SRS-179. Ashville, NC: United States Department of Agricultural Forest Service Research and Development, Southern Research Station. pp 11–26.

Woodall CW, Domke GM, Riley KL, Oswalt CM, Crocker SJ, Yohe GW. 2013. A framework for assessing global change risks to forest carbon stocks in the United States. PLoS ONE 8:e73222.

Yohe G. 2010. Risk assessment and risk management for infrastructure planning and investment. The bridge: linking engineering and society. Natl Acad Eng 40:14–21.

Yohe G, Leichenko R. 2010. Adopting a risk-based approach. Ann N Y Acad Sci 1196:29–40.